Comprehensive Exam Write-up: High and Low Fidelity Simulations of Compressible Supersonic Flow Around Complex Geometries

by

Nurlybek Kasimov

B.S., Moscow Institute of Physics and Technology, 2008

M.S., Moscow Institute of Physics and Technology, 2010

A thesis submitted to the

Faculty of the Graduate School of the

University of Colorado in partial fulfillment

of the requirements for the degree of

Doctor of Philosophy

Department of Mechanical Engineering

2014

This thesis entitled:
Comprehensive Exam Write-up: High and Low Fidelity Simulations of Compressible Supersonic Flow Around Complex Geometries
written by Nurlybek Kasimov
has been approved for the Department of Mechanical Engineering

Prof. Oleg V. Vasilyev

Prof. Peter Hamlington

Prof. Daven Henze

Prof. Alireza Doostan

Prof. Sedat Biringen

Prof. John A. Evans

Date

The final copy of this thesis has been examined by the signatories, and we find that both the content and the form meet acceptable presentation standards of scholarly work in the above mentioned discipline.

Kasimov, Nurlybek (Ph.D., Mechanical Engineering)

Comprehensive Exam Write-up: High and Low Fidelity Simulations of Compressible Supersonic Flow Around Complex Geometries

Thesis directed by Prof. Oleg V. Vasilyev

This work consist of two parts — high and low fidelity simulations of supersonic flow around solid obstacles of arbitrary shapes, accordingly. This project is supported by ONR MURI on Soil Blast Modeling. Low fidelity simulations were performed by solving 3D Euler equations for supersonic flows in presence of obstacles using Roe solver as a shock capturing scheme and modification of Brinkman penalization method to handle obstacles through forcing terms. Particle-particle interactions were handled using 3D DEM solver and then coupled with Euler/Roe CFD solver. High fidelity simulations, on the other hand, were performed using Adaptive Wavelet Collocation Method for grid adaptation and adaptive differentiation, Artificial Viscosity Method as a shock capturing scheme and Characteristic Based Volume Penalization Method to handle solid obstacles through forcing terms.

Contents

Chapter

Tables

Table

Figures

Figure

Chapter 1

Introduction

1.1 Motivation and Objective

This project is supported by ONR MURI on Soil Blast Modeling. It is a part of a bigger multiscale/multiphysics project on research and simulations of explosions of buried explosive devices [1]. In Figure 1.1 one can see ejecta under asphalt pavement after improvised explosive device (IED) explosion hitting U.S. military convoy, which was starting point of the project. Main motivation of the project is overcome wide variety of uncertainties that occur at the moment of explosion (blast wave propagation) due to the soil type, moisture, density; landmark peculiarities, explosive type, and etc., so one can better predict harmful effect of the explosion and perform a proper defensive strategies such as armoring.

Existing methodologies allow to do simulations on each peculiarity consisting this complex phenomenon separately but not for all of them simultaneously using coupled equations. The main focus of this project is to provide a low fidelity computation model of fluid-structure interaction of compressible supersonic flow around multiple solid particles. The model is based on high fidelity DNS simulations involving several orders of magnitude less number of particles and properly extrapolated and/or averaged in order to couple with other approaches. For that purpose new volume penalization method was developed for high fidelity simulations [2]. For low fidelity simulations volume penalization method roughly based on Brinkman method was developed, which

Figure 1.1: IED explosion in Iraq, hitting U.S. military convoy

mimicked boundary conditions on fluid-particle interface but which also took into the account extremely rough grid, i.e. boundary layer was not resolved.

1.2 Methodology

In this project several numerical techniques were used to address different parts of the framework. High fidelity simulations utilized Characteristic Based Volume Penalization (CBVP) method developed by O. V. Vasilyev, E. Brown-Dymkoski and N. Kasimov. To address discontinuities in flow parameters (shock waves) specific artificial viscosity method based on wavelets was used [3]. Local grid refinement (data compression) and corresponding differentiation on adaptive grid was achieved using Adaptive Wavelet Collocation Method (AWCM) [4]. Low fidelity simulations were performed using Briknman-like momentum penalization of Euler equations (inviscid flow) in order to match drag force. Riemann solver of Roe was used as a shock capturing scheme [5]. Particle-particle interaction was calculated using DEM/FEM method and later coupled with CFD part of the solver.

1.2.1 Volume penalization

In order to handle flows around solid obstacles numerically, several approaches are used. One can classify them into two main categories — Body Fitted Grid (BFG) methods and Immersed Boundary methods (IB) [6]. BFG methods allow to construct typically curvilinear grid in such a way that obstacle boundary is aligned with grid lines (See Figure. 1.2a), so no special treatment of the boundary conditions at the obstacle is needed.

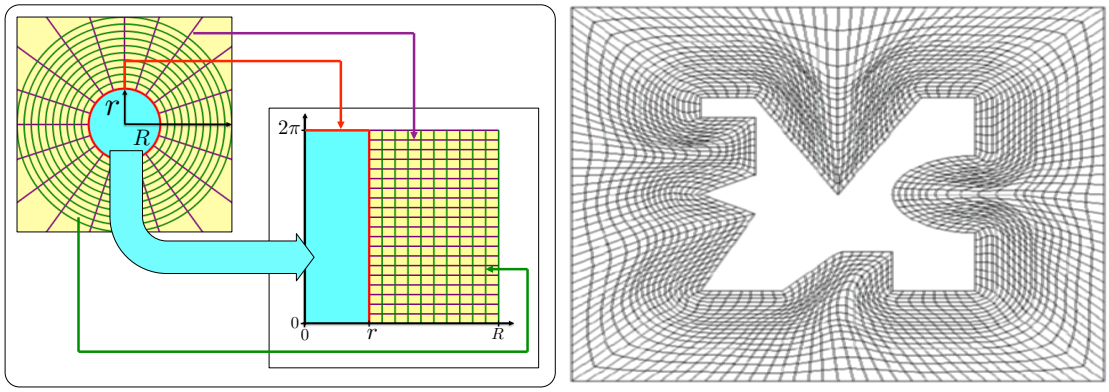

a) Circlualr object and grid lines b) More complex shape

Figure 1.2: Body fitted grid examples

In order to get rectilinear system as in Figure 1.2(a) one need to perform radial transformation

$$x = x_0 + r\cos\varphi$$

$$y = y_0 + r\sin\varphi$$

and change all equations accordingly. In most cases obstacles have more complex shapes (see Figure 1.2b) and finding corresponding transformation of the coordinates might be problematic. Additional difficulties arise when obstacle is allowed to move and deform due to the interaction with the flow — new transformation should be found at each time step.

IB methods, Volume Penalization (VP) methods in particular, in contrary, do

not change existing grid, but rather change governing equations, i.e. they are intrusive methods. Equations are modified through artificial forcing terms that are added to the governing equations so that solution at the boundary tends to the exact solution. The methodology underlying this project is a VP method.

1.2.1.1 Brinkman Penalization Method

The first VP method that was used at early stage of the project was Brinkman Penalization (BP) method, originally proposed by Arquis and Caltagirone [7] for incompressible flow around solid obstacles through momentum penalization. This method was successfully extended to the subsonic compressible flow [8]. The main advantages of the method are systematic error control and relative simplicity of numerical implementation. The very basic interpretation of the method can be achieved if one represents solid obstacle as a porous media with controlled permeability and porosity.

1.2.1.2 Characteristic Based Volume Penalization

BP method applied "as it is" to supersonic flows led to numerous errors, such as inaccurate acoustic reflection, pressure seepage, phase lag, etc. Also the fact that BP cannot be used to model boundary conditions other than Dirichlet and homogeneous Neuman made it difficult for some type of simulations with Neumann and Robin type boundary conditions. In order to handle these deficiencies new VP method was developed — Characteristic Based Volume Penalization. To mimic Dirichlet type boundary conditions CBVP still utilizes BP with some modifications to enhance numerical stability. For Neumann and Robin type boundary conditions the solution is propagated inside of the obstacle along inward directed normal vector, hence the name of the method.

1.2.1.3 Brikman-like Volume Penalization, Low Fidelity Simulations

For Lo-Fi simulations supersonic flow was modeled using extremely coarse grid. The latter restricted us to resolve boundary layer, so Euler equation were used instead. To mimic drag force caused by the flow as in case of the viscous flow, we introduced penalization of the momentum equation. Also, due to the coarse grid, in case of many obstacles amount of the flow penetrating the obstacle could lead to significant numerical errors. To fix it, another penalization terms related to the porosity was introduced, which is also inspired by BP method.

1.2.2 Adaptive Wavelet Collocation Method

In order to achieve data compression, i.e. to use fewer grid points than if one utilizes uniform rectangular grid, AWCM was used. The main advantage of the method is systematic a priori error control while maintaining structured rectilinear grid. Second generation interpolation wavelets were used as basis functions. Grid adaptation algorithm underlying the method allows to both accurately track regions of "important physics" and easily program it using existing numerical platforms. Tracking can be performed for dynamically changing phenomena without significant overhead — in many cases extra calculations are overcompensated by high data compression.

1.2.3 Shock Capturing Scheme

To handle discontinuities in Hi-Fi simulations, shock capturing scheme based on AWCM was used. It is based on the solution of hyperbolic equation near the discontinuities/shocks in order to smooth them with desired width. This procedure introduces non-linear artificial viscosity. The main reason to incorporate this method with AWCM is that latter serves as a good indicator of shock location through wavelet coefficients. Method exhibits good localization property, avoiding unnecessary smoothing in the regions where it is not required.

1.2.4 Shock Capturing Scheme, Low Fidelity Simulations

To handle discontinuities in Lo-Fi simulations Riemann solver of Roe was used. This method is equivalent to using artificial viscosity, although it cannot be controlled and viscosity value is defined by the flow. Main procedure underlying the method is performing certain type of averaging of flow parameters, so called Roe average. After the averaging, Euler equations become pseudo linear hyperbolic equations. Roe solver handles transonic and subsonic regions of the solution worse than discontinuities, although there are ways to overcome this issue, such as so called Harten-Hyman Entropy Fix.

1.2.5 CFD/DEM Coupling, Low Fidelity Simulations

In Lo-Fi simulations, due to the coarse CFD grid, it is possible to model supersonic flow around large number of particles that might interact with both flow and other particles. CFD-DEM coupling provides particle-particle and fluid-particle interactions, while CBVP provides particle-fluid interactions, closing the system. The only restriction applied to the system is to have same global time step for both CFD and DEM solvers, which in some cases might be inefficient.

1.3 Organization

The rest of this paper is organized as follows. In Chapter 2, the necessary background of Volume Penalization techniques, shock capturing schemes, Adaptive Wavelet transforms and basics of CFD-DEM coupling will be covered. Testing different numerical techniques with proper algorithm justification of chosen or developed algorithms is discusses in Chapter 3. In Chapters 4 and 5 one can find results of Hi-Fi and Lo-Fi simulations accordingly. Future work is presented in Chapter 6.

Chapter 2

Background

2.1 Brinkman Penalization

There are three main algorithmic steps involved in IB methods:

(1) Splitting mesh points into three classes (See Figure 2.1): Field points — points outside of the obstacle; Band points — field points closest to the obstacle surface; and Interior points — points inside of the obstacle.

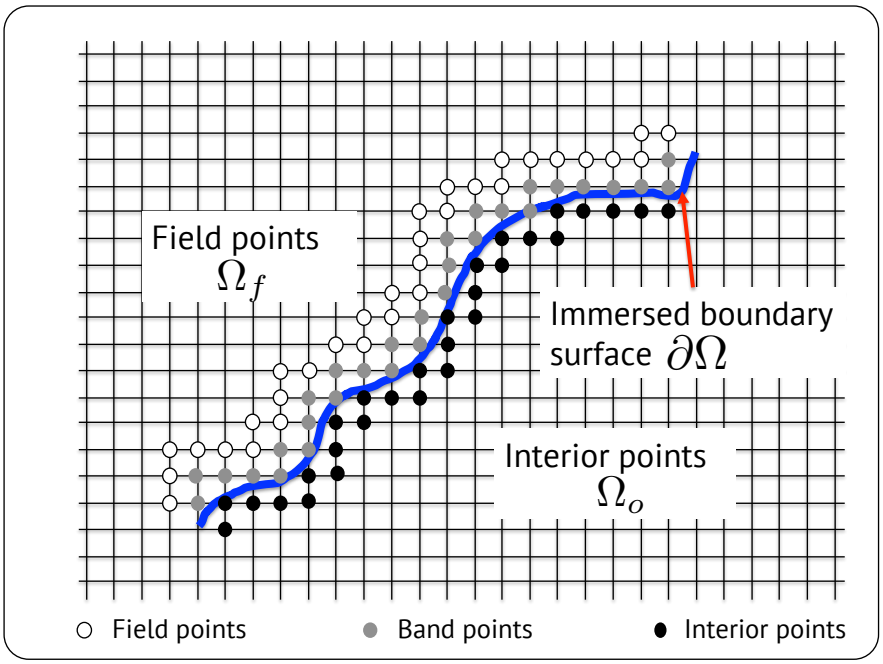

Figure 2.1: Mesh points for IB methods

(2) Introducing so-called Mask function, typically denoted as $\chi(\boldsymbol{x})$, which is nothing but indicator function

$$\chi(\boldsymbol{x}) = \begin{cases} 1, & \text{if } \boldsymbol{x} \in \Omega_o \\ 0, & \text{else.} \end{cases}$$

(3) Altering governing equations by adding forcing terms, so that boundary conditions at the obstacle surface are approximately satisfied, involving the $\chi(\boldsymbol{x})$ above, so that equations in field points do not change.

Additional forcing terms can be added either before the governing equations are discretized or after. This order determines the type of methods in IB methods family. Volume penalization (VP) is a subclass of IB methods where equations are altered before the discretization, therefore conceptually does not depend on numerical approach to be used.

Consider the following oversimplified version of Navier-Stokes equations

$$\begin{aligned} \frac{\partial \rho}{\partial t} + \frac{\partial \rho u_j}{\partial x_j} &= 0 \\ \frac{\partial \rho u_i}{\partial t} + \frac{\partial \rho u_i u_j}{\partial x_j} + \frac{\partial p}{\partial x_i} + \frac{\partial \tau_{ij}}{\partial x_j} &= 0 \\ \frac{\partial \rho e}{\partial t} + \frac{\partial u_j \left(\rho e + p\right)}{\partial x_j} + \frac{\partial u_i \tau_{ij}}{\partial x_j} &= 0, \end{aligned} \tag{2.1}$$

along with constitutive equations for ideal gas and Newtonian fluid assumption, that form a closed system.

Throughout entire writeup numerically more convenient form of the equations as described below will be used:

$$\frac{\partial \varphi}{\partial t} = RHS_{\varphi}. \tag{2.2}$$

The idea behind the Brinkman penalization is to alter momentum equation, i.e. penalize it, at every grid point, hence volume penalization.

$$\frac{\partial \rho u_i}{\partial t} = RHS - \frac{\chi}{\eta} \rho \left(u_i - U_i^o\right), \tag{2.3}$$

where η is numerical permeability of the obstacle. One needs to keep in mind that it is artificial. This equation, firstly, keeps solution outside of the obstacle unchanged due to the masking function and, secondly, mimics no slip boundary condition $u_i|_{\partial\Omega} = U_i^o$ after reaching steady state regime.

In order to reach proper acoustic reflection from the obstacle one can also introduce numerical porosity ϕ in continuity equation to mimic porous media in full extent.

$$\frac{\partial \rho}{\partial t} = -\frac{1}{\phi}\frac{\partial \rho u_j}{\partial x_j},$$

which can be translated to the form (2.2) as

$$\frac{\partial \rho}{\partial t} = RHS - \chi\left(\frac{1}{\phi} - 1\right)\frac{\partial \rho u_j}{\partial x_j}. \tag{2.4}$$

One can also penalize temperature as well, in case such boundary condition is meant to be satisfied at the obstacle boundary.

$$\frac{\partial T}{\partial t} = RHS - \frac{\chi}{\eta}\left(T - T^o\right), \tag{2.5}$$

which mimics isothermal boundary condition $T|_{\partial\Omega} = T^o$ and can be incorporated to the energy equation through the full energy relation for ideal gas,

$$\rho e = \frac{\rho u_j u_j}{2} + \rho c_V T = \frac{\rho u_j u_j}{2} + \frac{p}{\gamma - 1}. \tag{2.6}$$

Results of BP implementation to supersonic inviscid flow are shown in Chapter 3 as a motivation for new VP method.

2.2 Adaptive Wavelet Collocation Method

For Hi-Fi simulations to reduce number of used grid points AWCM was used. Let us consider some target function $u(\mathbf{x})$ that can be sampled on some uniform grid of chosen highest level of resolution, although grid does not have to be uniform, as long as it is structured. In this project uniform grid is used as a first step in grid adaptation.

Following Vasilyev et al. [4] one can decompose given function into wavelet functions and scaling function at the lowest level of resolution

$$u(\mathbf{x}) = \sum_{k \in \mathcal{K}^0} c_k^0 \phi_k^0(\mathbf{x}) + \sum_{j=0}^{\infty} \sum_{\mu=1}^{2^n-1} \sum_{l \in \mathcal{L}^{\mu,j}} d_l^{\mu,j} \psi_l^{\mu,j}(\mathbf{x}), \tag{2.7}$$

where $\phi_k^0(\mathbf{x})$ is a scaling function at the coarsest level of resolution and $\psi_l^{\mu,j}(\mathbf{x})$ is a wavelet function at the level of resolution j, c_k^0 and $d_l^{\mu,j}$ are scaling and wavelet coefficients accordingly. Main advantage of the decomposition above is it can be split into two parts

$$u(\mathbf{x}) = u_{\geq}(\mathbf{x}) + u_{<}(\mathbf{x}), \tag{2.8}$$

where

$$\begin{aligned} u_{\geq}(\mathbf{x}) &= \sum_{k \in \mathcal{K}^0} c_k^0 \phi_k^0(\mathbf{x}) + \sum_{j=0}^{\infty} \sum_{\mu=1}^{2^n-1} \sum_{\substack{l \in \mathcal{L}^{\mu,j} \\ \left|d_l^{\mu,j}\right| \geq \epsilon \|u\|}} d_l^{\mu,j} \psi_l^{\mu,j}(\mathbf{x}), \\ u_{<}(\mathbf{x}) &= \sum_{j=0}^{\infty} \sum_{\mu=1}^{2^n-1} \sum_{\substack{l \in \mathcal{L}^{\mu,j} \\ \left|d_l^{\mu,j}\right| < \epsilon \|u\|}} d_l^{\mu,j} \psi_l^{\mu,j}(\mathbf{x}), \end{aligned} \tag{2.9}$$

based on some threshold value ϵ. Donoho [9] had shown that absolute error of neglecting $u_{<}(\mathbf{x})$ part of the function leads to controllable error on the function, namely

$$\|u - u_{\geq}\| \leq C\epsilon \|u\|, \tag{2.10}$$

which means that one can use only part of the grid points and retain desired accuracy. This property allows to construct an adaptive grid with significantly fewer number of points. Only the regions with steep gradients have large values of wavelet coefficients, which makes wavelets a good indicator of those gradients. For example, in Fig. 2.2 wavelet coefficients of the function with two sharp transitions are presented.

Wavelet basis functions possess other "nice" properties, such as localization in both space and time. In this project, along with all other projects conducted in Multiscale Modeling and Simulation Laboratory led by Dr. Vasilyev, interpolating wavelets

are used (See Fig. 2.3). Constructing wavelet functions is relatively simple and have well described recursive algorithm [10].

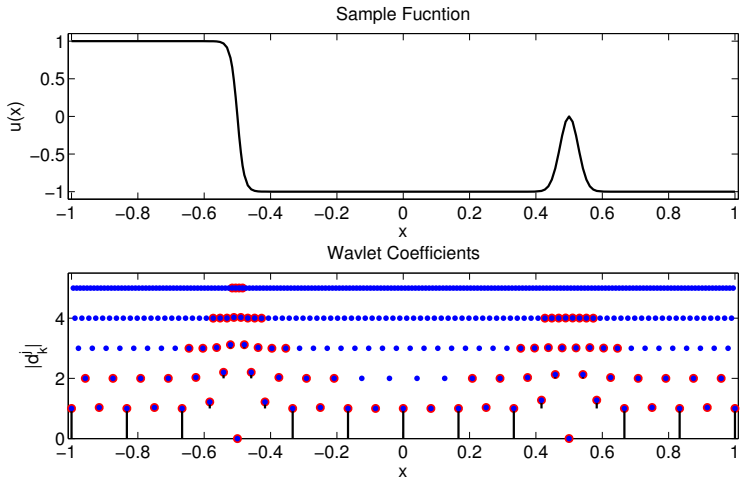

Figure 2.2: Wavelet coefficients of a function with two sharp transitions

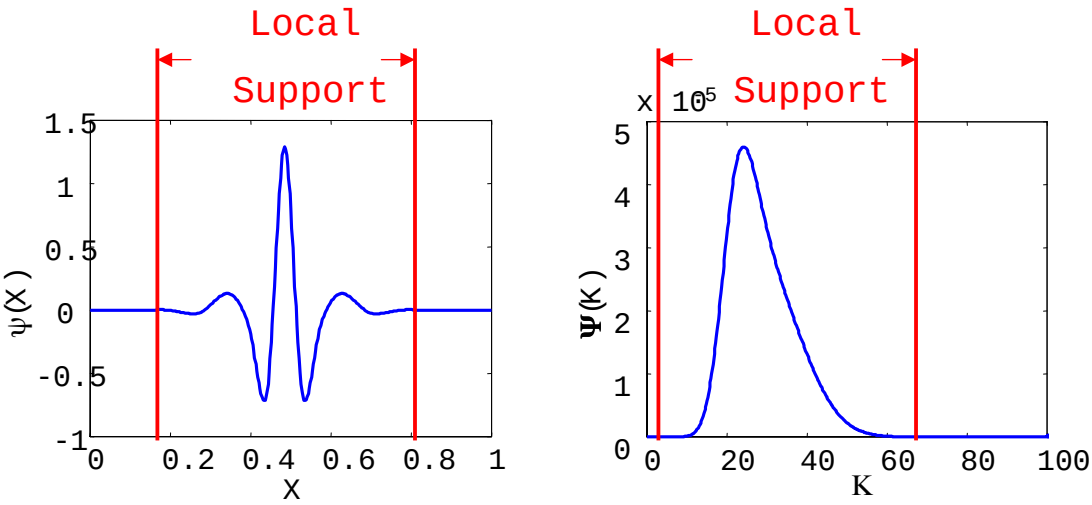

a) Interpolating wavelet of 3^{rd} order b) Fourier transform of wavelet

Figure 2.3: Localized nature of wavelet function

Adaptation procedure can be easily iterated over time evolution, which makes it also a dynamic, so one can assure that grid always represents current state of the physical phenomenon. In order to do this properly the concept of Adjacent Zone was introduced [4] (see Fig. 2.4). One may consider it as a safety regions within which

coefficients might become significant even after the time integration. In this case one can make sure that global accuracy of the simulations is still within the user defined and controlled threshold in evolution problems, and most importantly keep adapted grid in up to date state. Using adapted grid also saves memory required to store variable values at each grid point, since one needs fewer of them.

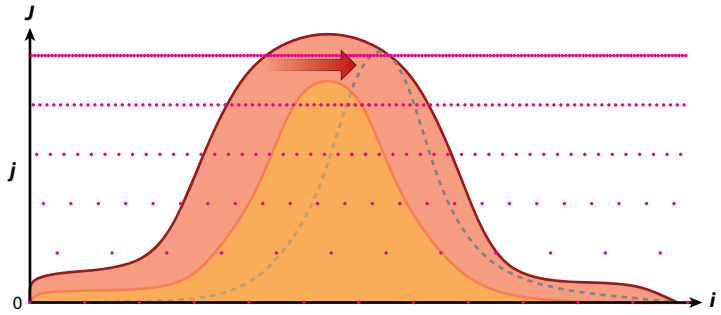

Figure 2.4: Safety region with possible significant wavelets after one time step

2.3 Wavelet Based Artificial Viscosity as a Shock Capturing Scheme

Using AWCM becomes even more attractive for Hi-Fi simulations per discussion in previous section — Wavelet coefficients have large values at the regions of steep gradients and discontinuities are as steep as one can get. Numerically it means that there are coefficients on all levels of resolution. By Regele and Vasilyev [3] was developed a method to track and smooth those gradients. The core of the method is to add artificial viscosity to the desired hyperbolic equation with dynamic artificial viscosity, when latter depends on "shock locator" — specifically cooked flux limiting function. Let us consider simple one dimensional conservation equation with added artificial diffusion term,

$$\frac{\partial u}{\partial t} + \frac{\partial f}{\partial x} = \frac{\partial}{\partial x}\left(\nu\left(\Phi\right)\frac{\partial u}{\partial x}\right), \tag{2.11}$$

where Φ can be found as

$$\Phi = \begin{cases} \frac{\left|d_k^{j_{max}}\right|}{\|u\|}, & \text{if } 0 < \left|d_k^{j_{max}}\right| \leq \epsilon_d \|u\| \\ 1, & \text{if } \left|d_k^{j_{max}}\right| > \epsilon_d \|u\|, \end{cases} \tag{2.12}$$

where $\left|d_k^{j_{max}}\right|$ is a wavelet coefficient at fines level of resolution and ϵ_d is also a chosen thresholding parameter to limit Φ, apart from the wavelet threshold parameter ϵ.

In Fig. 2.5 one may find viscosity field and corresponding Schlieren image of the density field for 2D supersonic flow around the solid circle. Problem was solved using aforementioned artificial viscosity. Per methods design, viscosity is non-zero at shock locations, based on the Schlieren image, and vanishes everywhere else.

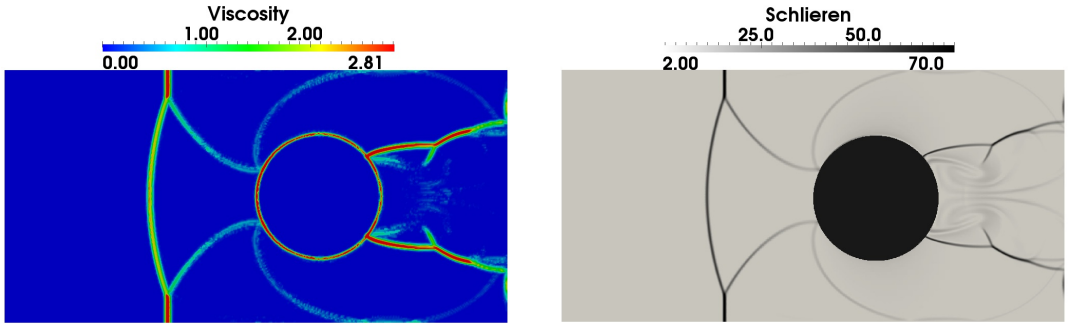

a) Viscosity field b) Schlieren image of the flow

Figure 2.5: Localized nature of wavelet function

2.4 Riemann Problem and Riemann Solver of Roe

A Riemann problem consists of a conservation laws together with piecewise constant data having a single discontinuity, or in other words, one or multiple hyperbolic equations with discontinuous initial conditions. As a such system one can consider Euler or Navier-Stokes equations. Either numerical or analytical technique to solve such a problem is called Riemann solver. For non-linear problems, like Euler and Navier-Stokes, there are number of numerical Riemann solvers, such as Godunov Scheme, Flux Vector Splitting, Roe solver [5], etc. For Lo-Fi simulations of this project latter was used.

For the sake of simplicity, let us consider pseudo one dimensional Euler equations for ideal gas with discontinuous ICs.

$$\begin{gathered}\frac{\partial \mathbf{u}}{\partial t}+\frac{\partial \mathbf{F}(\mathbf{u})}{\partial x}=0 \\ \mathbf{u}=\begin{cases}\mathbf{u}_L, & \text{if } x \leq x_S \\ \mathbf{u}_R, & \text{if } x>x_S,\end{cases}\end{gathered} \tag{2.13}$$

where

$$\mathbf{u}=\begin{bmatrix}\rho \\ \rho u \\ \rho v \\ \rho w \\ \rho e\end{bmatrix}, \qquad \mathbf{F}=\begin{bmatrix}\rho u \\ \rho u^2+p \\ \rho u v \\ \rho u w \\ u(\rho e+p)\end{bmatrix}, \tag{2.14}$$

and constitutive equation (2.6) to close the system. It can be rewritten in pseudo linear form

$$\frac{\partial \mathbf{u}}{\partial t}+\mathcal{A}(\mathbf{u})\frac{\partial \mathbf{u}}{\partial x}=0, \tag{2.15}$$

where $\mathcal{A}$ is a Jacobian matrix of the flux $\mathbf{F}$ with respect to the solution vector $\mathbf{u}$, which has the following explicit relation

$$\mathcal{A}=\begin{bmatrix}0 & 1 & 0 & 0 & 0 \\ \hat{\gamma}H-u^2-a^2 & (3-\gamma)u & -\hat{\gamma}v & -\hat{\gamma}w & \hat{\gamma} \\ -uv & v & u & 0 & 0 \\ -uw & w & 0 & u & 0 \\ u\left[(\gamma-2)H-a^2\right] & H-\hat{\gamma}u^2 & -\hat{\gamma}uv & -\hat{\gamma}uw & \gamma u\end{bmatrix}, \tag{2.16}$$

where $\hat{\gamma}=\gamma-1$, $H=(\rho e+p)/\rho$ (Specific enthalpy) and $a=\sqrt{\gamma p/\rho}$ (Local speed of sound). This matrix has eigenvalues

$$\lambda_1=u-a, \quad \lambda_2=\lambda_3=\lambda_4=u, \quad \lambda_5=u+a, \tag{2.17}$$

and eigenvectors

$$\left.\begin{aligned} \mathbf{K}^{(1)} = \begin{bmatrix} 1 \\ u-a \\ v \\ w \\ H-ua \end{bmatrix}, \mathbf{K}^{(2)} = \begin{bmatrix} 1 \\ u \\ v \\ w \\ \frac{1}{2}V^2 \end{bmatrix}, \mathbf{K}^{(3)} = \begin{bmatrix} 0 \\ 0 \\ 1 \\ 0 \\ v \end{bmatrix}, \\ \mathbf{K}^{(4)} = \begin{bmatrix} 0 \\ 0 \\ 0 \\ 1 \\ w \end{bmatrix}, \mathbf{K}^{(5)} = \begin{bmatrix} 1 \\ u+a \\ v \\ w \\ H+ua \end{bmatrix} \end{aligned}\right\}, \tag{2.18}$$

where $V = \left(u^2 + v^2 + w^2\right)$.

Equation (2.15) can be numerically integrated as

$$\mathbf{u}_i^{n+1} = \mathbf{u}_i^n + \frac{\Delta t}{\Delta x}\left(\mathbf{F}_{i-\frac{1}{2}} - \mathbf{F}_{i+\frac{1}{2}}\right), \tag{2.19}$$

where half-integer indices are introduced for convenience and to distinguish intercell values from cell values on chosen grid. Variety of Riemann solvers differ by the way they calculate those intercell values.

Philip Roe proposed to calculate intercell fluxes using certain averaging procedure based on right and left values of corresponding local fluxes [11] as follows

$$\widetilde{(\bullet)} = \frac{\sqrt{\rho_L}\,(\bullet)_L + \sqrt{\rho_R}\,(\bullet)_R}{\sqrt{\rho_L} + \sqrt{\rho_R}}\ , \tag{2.20}$$

where $(\bullet)$ stands for u, v, w and H. After finding these averaged values, one also needs to find $\widetilde{V}$ and $\widetilde{a}$ as

$$\begin{aligned} \widetilde{V} &= \widetilde{u}^2 + \widetilde{v}^2 + \widetilde{w}^2, \\ \widetilde{a} &= \left[\hat{\gamma}\left(\widetilde{H} - \frac{1}{2}\widetilde{V}^2\right)\right]^{\frac{1}{2}}. \end{aligned}$$

Next step is to substitute all values defined in (2.16)-(2.18) with averaged values. Finally, according to Roe, intercell flux can be found as

$$\mathbf{F}_{i+\frac{1}{2}} = \frac{1}{2}\left(\mathbf{F}_L + \mathbf{F}_R\right) - \frac{1}{2}\sum_{j=1}^{5} \widetilde{\alpha}_j \left|\widetilde{\lambda}_j\right| \widetilde{\mathbf{K}^j}, \tag{2.21}$$

where α_j is so called wave strength — weight that takes into account contribution from each eigenvector. Roe's original approach is to calculate them as follows:

$$\begin{aligned}
\widetilde{\alpha}_3 &= \Delta u_3 - \widetilde{v}\Delta u_1, \\
\widetilde{\alpha}_4 &= \Delta u_4 - \widetilde{w}\Delta u_1, \\
\widetilde{\alpha}_2 &= \frac{\hat{\gamma}}{\widetilde{a}^2}\left[\Delta u_1\left(\widetilde{H} - \widetilde{u}^2\right) + \widetilde{u}\Delta u_2 - \overline{\Delta u_5}\right], \\
\widetilde{\alpha}_1 &= \frac{1}{2\widetilde{a}}\left[\Delta u_1\left(\widetilde{u} + \widetilde{a}\right) - \Delta u_2 - \widetilde{a}\widetilde{\alpha}_2\right], \\
\widetilde{\alpha}_5 &= \Delta u_1 - \left(\widetilde{\alpha}_1 + \widetilde{\alpha}_2\right),
\end{aligned} \tag{2.22}$$

where $\Delta\mathbf{u} = \mathbf{u}_R - \mathbf{u}_L$ and $\overline{\Delta u_5} = \Delta u_5 - \widetilde{\alpha}_3\widetilde{v} - \widetilde{\alpha}_4\widetilde{w}$. $\mathbf{u}$ — is a solution vector. This procedure can be naturally extended to the full 3D case, with simple directional rotation of coordinate system and considering each direction as flow direction in pseudo one dimensional problem.

Chapter 3

New Volume Penalization Methods

3.1 Brinkman-like Penalization for Low Fidelity Simulations

Due to the coarse grid used in Lo-Fi simulations slightly modified BP methods was developed, in order to match drag force that drives particles obtained numerically with experimental results. The idea is to introduce momentum penalization term which is quadratic in velocity

$$\frac{\partial \rho u_i}{\partial t} = RHS - \frac{\chi}{\eta}\rho\left(u_i - U_i^o\right)^2. \tag{3.1}$$

From one hand, it forces the solution to the proper value at the obstacle boundary even faster than in case of simple BP, on the other hand this expression makes modeling of the penalization easier and flow independent. Namely,

$$F_{drag} = \int\limits_{\Omega} \frac{1}{\eta}\rho\left(u - U^o\right)^2 \; dV \sim \int\limits_{A} \frac{1}{2}\rho C_d \left(u - U^o\right)^2 \; dA, \tag{3.2}$$

where Ω is the volume of the obstacle, and A is largest cross section are across the flow and χ is dropped since integration is performed only inside of the obstacle. For the sake of simplicity, let us consider uniform flow around triaxial ellipsoid with semi axes a, b and c. In that case $\Omega = \pi abc$ and $A = \pi ab$, under the assumption that flow goes along c semi axis. So, (3.2) simplifies into

$$\frac{\pi abc}{\eta} \sim \frac{1}{2}\pi ab \; C_d \implies \eta \sim \frac{c}{2C_d}. \tag{3.3}$$

3.2 Characteristic Based Volume Penalization

First VP method used in Hi-Fi simulations was Brinkman Penalization. For testing purposes 1D Riemann problem for Euler equations were solved (see Fig. 3.1).

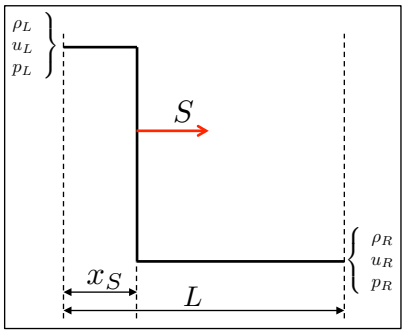

Figure 3.1: Riemann problem set up

To compare results, first, normal self-sustained shock problem was solved with reflection on the right domain boundary. Then right domain was extended and part of the domain was considered as solid obstacle and BP was used to model that solid obstacle/wall. Results revealed that using BP without any modification to supersonic flow leads to significant numerical errors such as phase lag and amplitude error, e.g. pressure seepage (see Fig. 3.2).

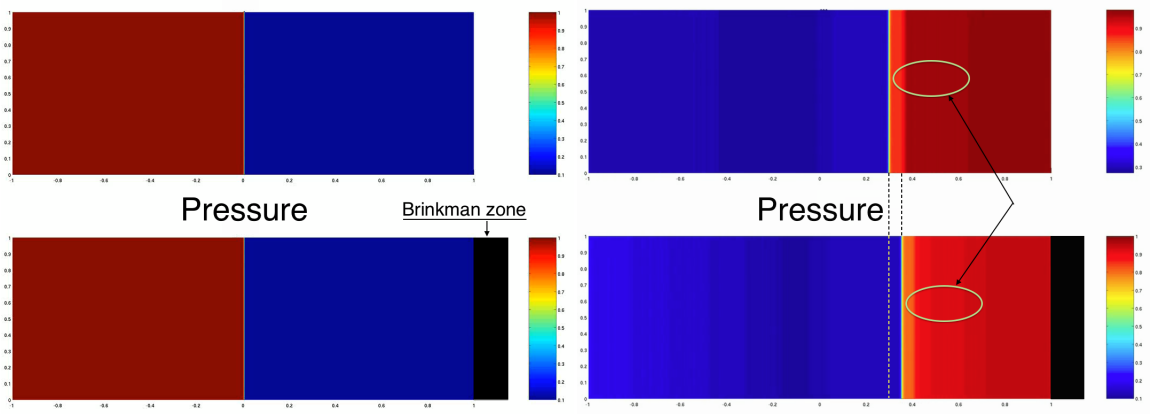

a) Initial condition of SOD1 test b) End state of SOD1 test

Figure 3.2: Normal reflection from the wall (top) and BP (bottom)

In order to overcome deficiencies of BP regarding flow regimes and boundary conditions, new VP method was developed. Let us consider general BC that one wants to mimic at the fluid-solid interface

$$\mathcal{L}(\bullet) = f_{boundary}, \tag{3.4}$$

where $(\bullet)$ may stand for any of the integrated variables, and operator $\mathcal{L}$ can describe either Dirichlet or Neumann boundary conditions, or Robin type BC. The idea is to replace evolution problem under the consideration as follows:

$$\frac{\partial \phi}{\partial t} = RHS \longrightarrow \frac{\partial \phi}{\partial t} = (1-\chi)RHS - \frac{\chi}{\eta}\left[\mathcal{L}(\phi) - f_{boundary}\right]. \tag{3.5}$$

Obviously, BP method is a special case of CBVP, when $\mathcal{L} = \mathbb{1}$ and $f_{boundary} = U^o$ for velocity or $f_{boundary} = T^o$ for temperature. Let us consider the same Riemann problem, but using the following BC at the obstacle instead:

$$\left.\begin{aligned} u_i^n|_{\partial\Omega} &= U_i^{on} \\ \left.\frac{\partial u_i^\tau}{\partial n}\right|_{\partial\Omega} &= 0 \\ \left.\frac{\partial p}{\partial n}\right|_{\partial\Omega} &= 0 \end{aligned}\right\}, \tag{3.6}$$

where $u_i^n = u_j n_j n_i$ is a normal component of the velocity, $u_i^\tau = u_i - u_i^n$ is a tangental component and $\partial/\partial n \equiv n_j \partial/x_j$ is a derivative in normal direction.

According to (3.5) evolution equations need to be changed as described below:

$$\left\{\begin{aligned} \frac{\partial u_i^n}{\partial t} &= (1-\chi)RHS - \frac{\chi}{\eta_b}(u_i^n - U_i^{on}) \\ \frac{\partial u_i^\tau}{\partial t} &= (1-\chi)RHS - \frac{\chi}{\eta_c}\frac{\partial u_i^\tau}{\partial n} \\ \frac{\partial p}{\partial t} &= (1-\chi)RHS - \frac{\chi}{\eta_c}\frac{\partial p}{\partial n}, \end{aligned}\right.$$

which can be translated to the equations in terms of integrated variables (with omitted

outside-of-the-obstacle part),

$$\begin{cases} \dfrac{\partial \rho}{\partial t} &= -\dfrac{1}{\eta_c}\dfrac{\partial \rho}{\partial n} \\ \dfrac{\partial \rho u_i^n}{\partial t} &= -\dfrac{1}{\eta_b}\rho\left(u_i^n - U_i^{on}\right) + \nu_n \Delta u_i^n \\ \dfrac{\partial \rho u_i^\tau}{\partial t} &= -\dfrac{1}{\eta_c}\dfrac{\partial \rho u_i^\tau}{\partial n} \\ \dfrac{\partial \rho e}{\partial t} &= -\dfrac{1}{\eta_c}\dfrac{\partial \rho e}{\partial n} - \dfrac{1}{\eta_b}\rho u_j^n\left(u_j^n - U_j^{on}\right) + \dfrac{1}{\eta_c}u_j^n\dfrac{\partial \rho u_j^n}{\partial n} + u_j^n \nu_n \Delta u_j^n. \end{cases} \tag{3.7}$$

One can notice that in (3.7) there are extra terms in energy equation. They appear due to the fact that there is no so called "characteristic term" in normal momentum penalization and one need to add it and subtract in order to have characteristic term in energy equation as well. Also, extra diffusive term was added to the same normal momentum equation to enhance stability. These technique resulted improvements in comparison to regular BP method (see Fig. 3.3). One can find more results on using CBVP for variety of problems in Chapter 4, as well as benchmarks.

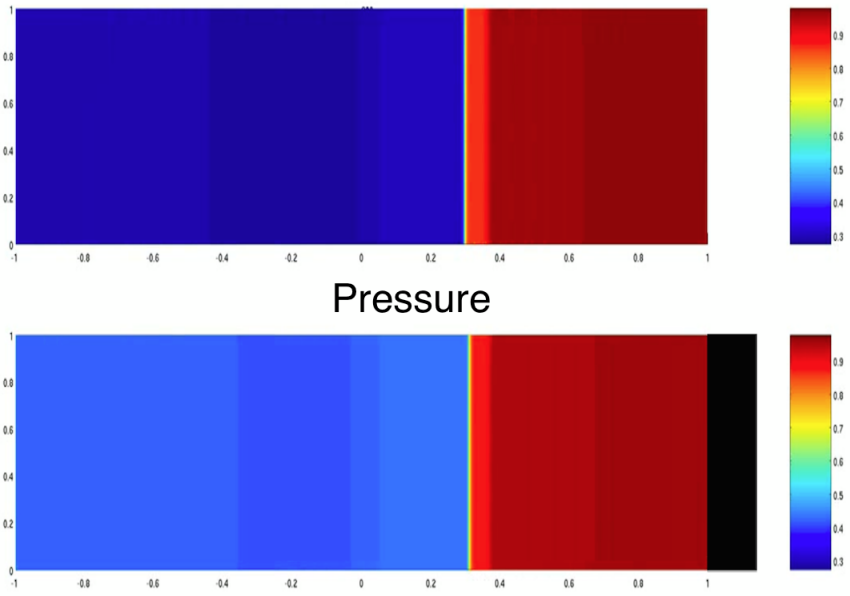

Figure 3.3: SOD1 test problem with CBVP

Chapter 4

High Fidelity Simulation Results

In this chapter one can find the results of benchmarking for CBVP applied to simple testing problem — Heat equation with different boundary conditions at the wall (Dirichlet, Neumann, Robin), as well as results of Hi-Fi simulations with the use of CBVP for flows around different number and types of obstacles.

4.1 Benchmark of using Characteristic Based Volume Penalization

Applicability of CBVP on different BC was tested on 1D heat equation (4.1).

$$\frac{\partial T}{\partial t} = k\frac{\partial^2 T}{\partial x^2}. \tag{4.1}$$

On the right domain boundary the wall was placed, so one can observe reflection of the incident wave using CBVP and compare it to exact solution. The main error controlling parameter in CBVP is penalization parameter η, so it was varied to achieve convergence with exact solution.

4.1.1 Dirichlet Boundary Condition

This boundary condition (4.2), also called isothermal boundary condition, specifies temperature (integrated variable for heat equation) as a constant value at the obstacle/wall interface. In this particular benchmark the value was equal to 0.

$$T|_{wall} = 0 \qquad \Longrightarrow \qquad \frac{\partial T}{\partial t} = k\frac{\partial^2 T}{\partial x^2} - \frac{\chi}{\eta_b} T. \tag{4.2}$$

Varying penalization parameter η_b led to solutions with different accuracy (see Fig. 4.1).

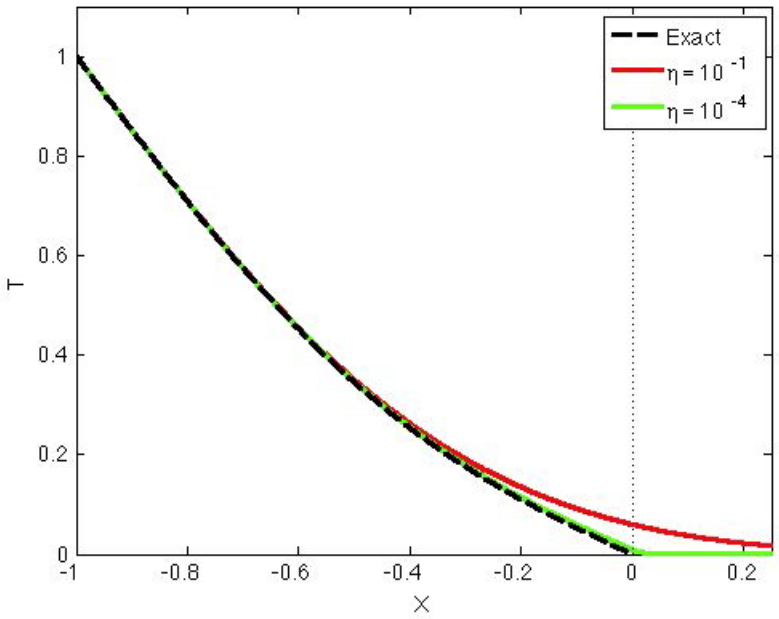

Figure 4.1: Temperature profile at the end of simulation. Dirichlet boundary condition.

One can see that $\eta_b = 10^{-4}$ converges to the exact solution well. In fact, rate of convergence for this simulation is $\sqrt{\eta_b}$ [2], since it is Brinkman type penalization [8].

4.1.2 Neumann Boundary Condition

This boundary condition (4.3) specifies constant rate of heat amount going in to or out of the system. In case of zero rate it is called adiabatic boundary condition. In this benchmark latter was considered.

$$\left.\frac{\partial T}{\partial x}\right|_{wall} = 0 \qquad \Longrightarrow \qquad \frac{\partial T}{\partial t} = (1-\chi)k\frac{\partial^2 T}{\partial x^2} - \frac{\chi}{\eta_c}\frac{\partial T}{\partial x}. \tag{4.3}$$

Analogously to Dirichlet BC, varying penalization parameter η_c led to different accuracy of the solution (see Fig. 4.2). Rate of convergence for this type of simulations is η_c [2]. One can notice that penalization parameter for Neumann type BC is different than for

Dirichlet type BC, which is connected to different time scales of the processes. In case of BP solution at the boundary decays inside of the obstacle, on the other hand for characteristic BC solution is translated inside of the obstacle.

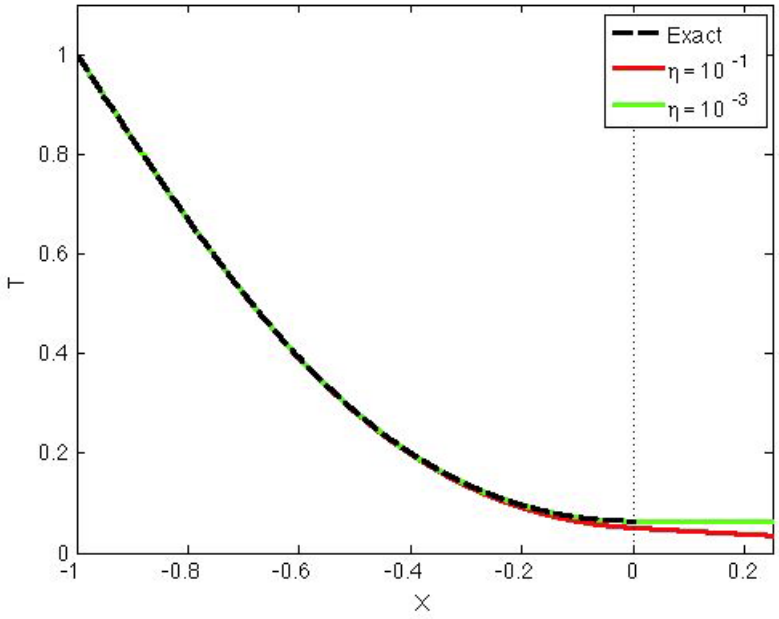

Figure 4.2: Temperature profile at the end of simulation. Neumann boundary condition.

4.1.3 Robin Boundary Condition

Last benchmark problem was to mimic Robin boundary condition at the obstacle interface, when both the solution value and its derivative are specified at the boundary. In this particular problem (4.4) was used as a BC.

$$T + 2\frac{\partial T}{\partial x} = 5 \qquad \Longrightarrow \qquad \frac{\partial T}{\partial t} = (1-\chi)k\frac{\partial^2 T}{\partial x^2} - \frac{\chi}{\eta_r}\left(T + 2\frac{\partial T}{\partial x} - 5\right). \tag{4.4}$$

In this type of simulations rate of convergence was predominated due to characteristic based terms as η_r [2] (see Fig. 4.3).

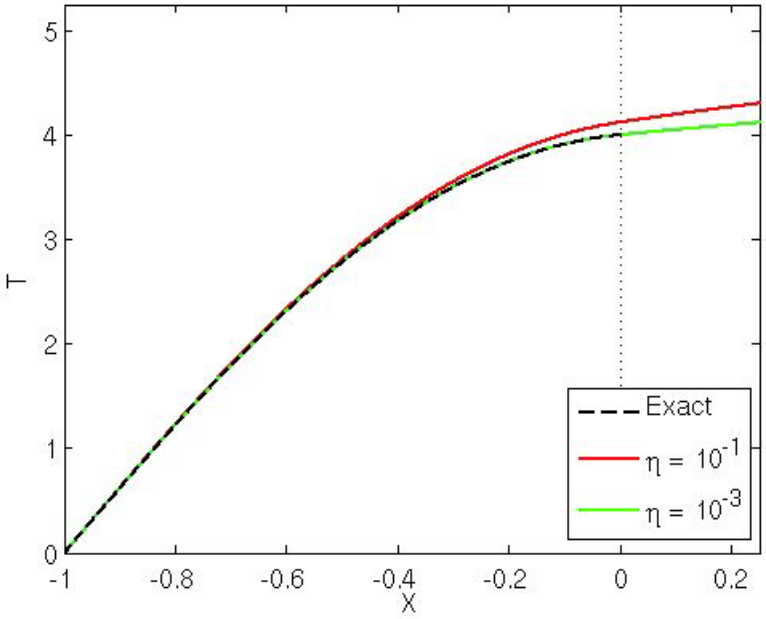

Figure 4.3: Temperature profile at the end of simulation. Robin boundary condition.

4.2 Simulation Results

After the method was validated and convergence rates were studied, variety of 2D simulations of supersonic inviscid flow were performed. Namely, flow around single and multiple stationary and moving cylinders, wedges with subcritical and supercritical angles. It is worth to mention that at this point no quantitative analysis of applicability of CBVP was done for these simulations. All results are treated based on the assumption that convergence rates defined in heat equation benchmarks hold for these simulations according to the used BCs (either $\sim \sqrt{\eta}$ or $\sim \eta$).

4.2.1 Flow Around the Wedge

In this set of simulations supersonic flow around both subcritical and supercritical wedges are considered. Incident shock speed is $M = 1.5$ (see Fig. 4.4). In case of subcritical wedge, i.e. angle at the apex is less than certain critical angle θ_{crit}, secondary oblique shock is performed.

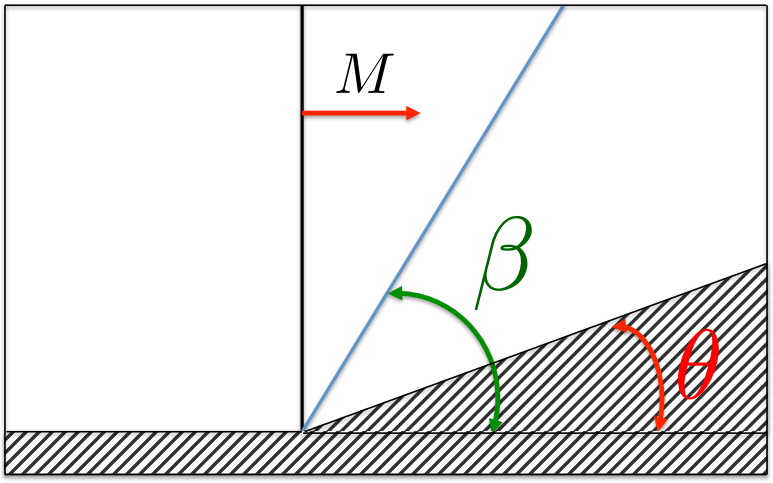

Figure 4.4: Schematic of the flow around the wedge.

Between the wedge angle θ and oblique shock deflection angle β there is a relation called "$\theta - \beta - M$" equation (4.5) (see Fig. 4.5).

$$\tan\theta = 2\cot\beta \frac{M\sin^2\beta - 1}{M^2(\gamma + \cos 2\beta) + 2}. \tag{4.5}$$

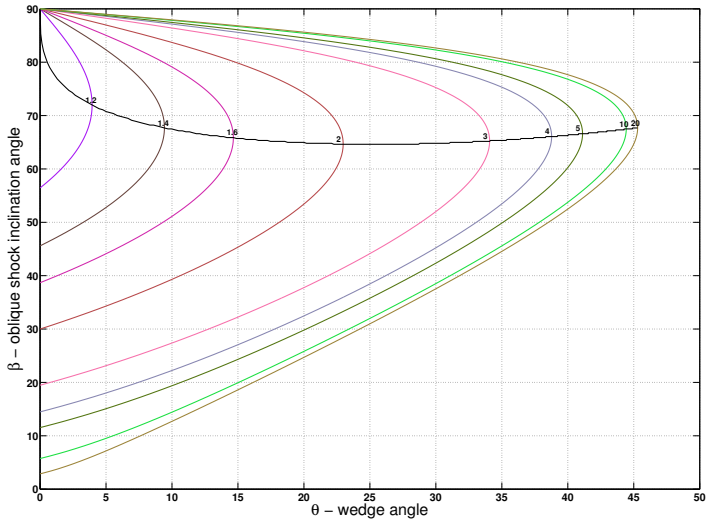

Figure 4.5: $\theta - \beta - M$ relation plot.

For this particular setup, one can find that $\theta_{crit} \approx 15°$, and subcritical wedge angle was

$\theta = 10°$. For the wedge angle $\theta > \theta_{crit}$ detached bow shock is formed. Supercritical angle was $\theta = 25°$.

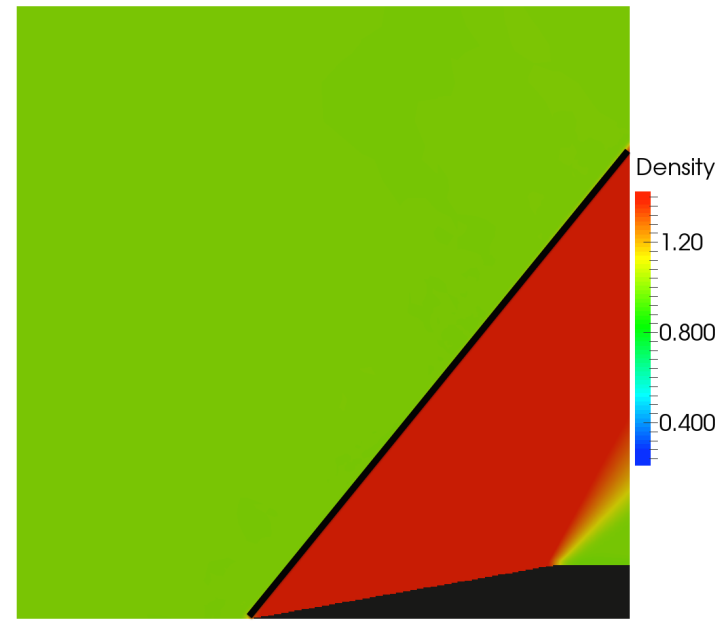

Subcritical wedge

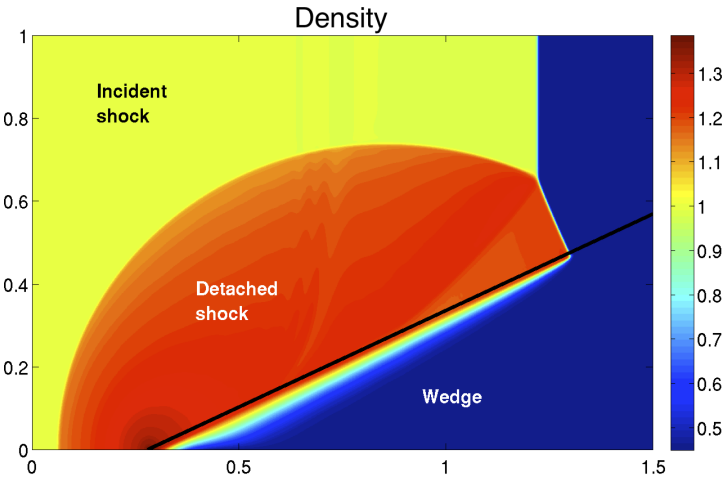

Supercritical wedge

Figure 4.6: Flow around the wedge results.

4.2.2 Flow Around Single and Multiple Stationary Cylinders

In this set of simulations, same $M = 1.5$ shock impinges either single or multiple solid cylinders (see Fig. 4.7). Unlike the flow around the wedge, in case of cylinder

always detached shock will be formed. There is no analytical solution to this problem, although plenty of both experimental and numerical results.

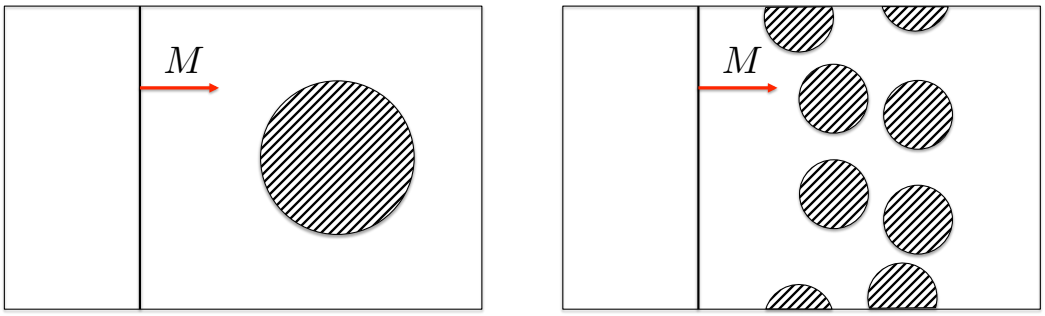

Figure 4.7: Single and multiple cylinders case schematics

All of our results here, for cylinders, wedge, etc, split by subsections

Chapter 5

Low Fidelity Simulation Results

Some low fidelity results of simulations we made with beichuan here. Probably some subsection on two-way coupling too.

Chapter 6

Future Work

Still working on future work part. Will be about making 3D simulations, getting better models to apply in Lo-Fi simulations.

Bibliography

[1] R. Regueiro and et.al., "Onr muri project on soil blast modeling and simulation," in Dynamic Behavior of Materials (B. Sang, D. Casem, and J. Kimberley, eds.), vol. 1 of Society for Experimental Mechanics Series, (Bethel, CT, USA), pp. 341–353, Society for Experimental Mechanics, Inc., Springer, 2014.

[2] E. Brown-Dymkoski, N. Kasimov, and O. V. Vasilyev, "A characteristic based volume penalization method for general evolution problems applied to compressible viscous flows," J. Comp. Phys., vol. 262, pp. 344–357, April 2014.

[3] J. Regele and O. Vasilyev, "An adaptive wavelet-collocation method for shock computations," Intl. Journal of CFD, vol. 23, no. 7, pp. 503–518, 2009.

[4] K. Schneider and O. V. Vasilyev, "Wavelet methods in computational fluid dynamics," Ann. Rev. Fluid Mech., vol. 42, pp. 473–503, 2010.

[5] E. Toro, Riemann Solvers and Numerical Methods for Fluid Dynamics: A Practical Introduction. Springer, 3 ed., 2009.

[6] C. Peskin, "Numerical analysis of blood flow in the heart," J. Comp. Phys., vol. 25, no. 3, pp. 220–252, 1977.

[7] E. Arquis and J. Caltagirone, "Sur les conditions hydrodynamiques au voisinage d'une interface milieu fluide – milieu poreux: application à la convection naturelle," C.R. Acad. Sci. Paris II, vol. 299, pp. 1–4, 1984.

[8] Q. Liu and O. Vasilyev, "A brinkman penalization method for compressible flows in complex geometries," J. Comp. Phys., vol. 227, no. 2, pp. 946–966, 2007.

[9] D. L. Donoho, "Interpolating wavelet transforms," tech. rep., Department of Statistics, Stanford University, October 1992.

[10] W. Sweldens and P. Shroder, Wavelets in the Geosciences, vol. 90 of Lecture Notes in Earth Sciences, ch. 2, pp. 72–107. Springer, 2000.

[11] P. Roe, "Approximate riemann solvers, parameter vectors, and difference schemes," J. Comp. Phys., vol. 43, no. 2, pp. 357–372, 1981.